A crucial role for Mim2 in the biogenesis of mitochondrial outer membrane proteins

Kai S. Dimmer[1], Dražen Papić[1], Benjamin Schumann[1,*], Desirée Sperl[1], Katrin Krumpe[1], Dirk M. Walther[2] and Doron Rapaport[1,‡]

[1]Interfaculty Institute of Biochemistry, University of Tübingen, 72076 Tübingen, Germany
[2]Max Planck Institute of Biochemistry, 82152 Martinsried, Germany

[*]Present address: Max Planck Institute for Colloids and Interfaces, 14476 Potsdam, and Free University Berlin, 14195 Berlin, Germany
[‡]Author for correspondence (doron.rapaport@uni-tuebingen.de)

Accepted 12 March 2012
Journal of Cell Science 125, 3464–3473

doi: 10.1242/jcs.103804

Summary

Most of the mitochondrial outer membrane (MOM) proteins contain helical transmembrane domains. Some of the single-span proteins and all known multiple-span proteins are inserted into the membrane in a pathway that depends on the MOM protein Mitochondrial Import 1 (Mim1). So far it has been unknown whether additional proteins are required for this process. Here, we describe the identification and characterization of Mim2, a novel protein of the MOM that has a crucial role in the biogenesis of MOM helical proteins. Mim2 physically and genetically interacts with Mim1, and both proteins form the MIM complex. Cells lacking Mim2 exhibit a severely reduced growth rate and lower steady-state levels of helical MOM proteins. In addition, absence of Mim2 leads to compromised assembly of the translocase of the outer mitochondrial membrane (TOM complex), hampered mitochondrial protein import, and defects in mitochondrial morphology. In summary, the current study demonstrates that Mim2 is a novel central player in the biogenesis of MOM proteins.

Key words: Mim2, MIM complex, Mitochondria, Outer membrane, Protein import

Introduction

The mitochondrial outer membrane (MOM) harbors a diverse set of proteins with functions ranging from biosynthetic pathways, morphogenesis and inheritance of the organelle to protein import into mitochondria (Burri et al., 2006; Schmitt et al., 2006; Zahedi et al., 2006). As all MOM proteins are encoded in the nucleus and translated on ribosomes in the cytosol, they have to be targeted to the organelle and inserted into the membrane (Neupert and Herrmann, 2007; Chacinska et al., 2009; Endo and Yamano, 2009; Walther and Rapaport, 2009). Despite recent progress, the various insertion mechanisms by which MOM proteins are incorporated into the membrane are still poorly understood.

MOM proteins can be divided according to their topologies into different families (Dukanovic and Rapaport, 2011). The β-barrel proteins form one family and are unique to the outer membranes of chloroplasts, mitochondria and Gram-negative bacteria. Their mitochondrial import route via the dedicated complex for topogenesis of outer membrane beta-barrel proteins (TOB), also known as sorting and assembly machinery (SAM) complex, is the best studied among the MOM proteins. Three additional protein families contain a single helical transmembrane domain (TMD). The so called tail-anchored (TA) and signal-anchored (SA) proteins bear this domain at their very C- or N-terminus, respectively (Wattenberg and Lithgow, 2001; Waizenegger et al., 2003; Ahting et al., 2005). An additional group is comprised of proteins that contain a central TMD, thus exposing domains to both the cytosol and the intermembrane space (IMS). Finally, a unique group is composed of MOM proteins that transverse the membrane via multiple helical TMDs.

The import pathways of helical MOM proteins are ill defined. Some evidence exists that tail- and signal-anchored proteins insert into the MOM without participation of a dedicated insertion machinery (Setoguchi et al., 2006; Kemper et al., 2008; Meineke et al., 2008). Other reports suggest a partial overlap in insertion pathways of polytopic and TA proteins (Rojo et al., 2002; Otera et al., 2007).

Two recent reports shed new light on the insertion mechanism of multispan proteins. They demonstrate that the outer membrane protein Mitochondrial Import 1 (Mim1) plays a crucial role in the insertion of multispan MOM proteins (Becker et al., 2011; Papic et al., 2011). The results suggest that precursor proteins are first recognized by Tom70 and then handed over to a Mim1-containing complex. Mim1 was originally identified in a systematic screen as a mutant that accumulates mitochondrial precursor proteins. It is a small integral protein of the MOM with a molecular mass of roughly 13 kDa (Mnaimneh et al., 2004; Dimmer and Rapaport, 2010). Later studies reported that Mim1 is a component of a higher molecular weight complex and that the protein is necessary for biogenesis of Tom20 and Tom70 and therefore also for the assembly of the TOM complex (Ishikawa et al., 2004; Waizenegger et al., 2005; Becker et al., 2008; Hulett et al., 2008; Popov-Celeketić et al., 2008; Lueder and Lithgow, 2009; Becker et al., 2010; Thornton et al., 2010).

Whereas the involvement of Mim1 in the biogenesis of outer membrane (OM) helical proteins is well documented, it has been unclear so far whether additional proteins are required for this process. Furthermore, the actual composition of the Mim1-containing complex and its mode of function are still unknown. Here, we report on the identification and characterization of a novel outer membrane protein, Mim2 that is crucial for proper growth of yeast cells. Mim2 and Mim1 are components of the same functional

complex that is playing a central role in the biogenesis of MOM proteins.

Results

Identification of Mim2

Mim1 was reported to be a subunit of a higher molecular weight complex of unknown composition. To search for additional components of the Mim1-containing complex, we performed immunoprecipitation in combination with stable isotope labeling with amino acids in cell culture (SILAC) (Ong et al., 2002). This method has been widely used to identify protein-protein interactions (Selbach and Mann, 2006; Hubner et al., 2010; Vermeulen et al., 2010; Walther and Mann, 2010). Mitochondria were isolated from a *mim1*Δ strain transformed with a vector encoding either Mim1 or GFP–Mim1, organelles were lysed with digitonin, and the lysate was incubated with beads specifically binding GFP. Bound material was digested with the protease LysC and resulting peptides were analyzed by high-resolution mass spectrometry followed by data processing with the MaxQuant software environment (Cox and Mann, 2008). Among the identified proteins particularly the putative open reading frame (ORF) *YLR099W-A* displayed an enrichment very similar to that of the bait protein Mim1 (supplementary material Fig. S1). Due to its identification as an interaction partner of Mim1, we named this ORF *MIM2*. According to the Saccharomyces Genome Database (SGD, www.yeastgenome.org), this small ORF is an essential gene and encodes a protein of 87 amino acids. Mim2 has no homologs in higher eukaryotes but is conserved in fungi like *Schizosaccharomyces pombe* and *Neurospora crassa* (Fig. 1A). Although several hydrophobic amino acids are clustered in the middle of the primary sequence (Fig. 1A), no transmembrane domain was predicted by commonly used programs.

Mim2 is an integral protein of the MOM

To investigate the subcellular localization of Mim2, yeast cells deleted for the chromosomal copy of *MIM2* were transformed with a vector encoding either native Mim2 or Mim2 with a C-terminal HA-tag. Both Mim2 and Mim2–HA expressed in this way were functional as they rescued the growth defect of *mim2*Δ cells (supplementary material Fig. S2 and text below). Subcellular fractionation demonstrated that Mim2–HA is present in the mitochondrial fraction (Fig. 1B). Next, we subjected mitochondria harboring Mim2–HA to an alkaline extraction treatment in which soluble and peripheral membrane proteins can be separated from integral membrane proteins by centrifugation. As shown in Fig. 1C, Mim2–HA, like the integral membrane protein Tom40, was enriched in the pellet fraction, suggesting that Mim2 is a mitochondrial membrane protein.

Since mitochondria have two distinct membranes, we wanted to investigate in which membrane Mim2 is located and study its membrane topology. Mitochondria containing Mim2–HA were either left intact or their OM was ruptured under hypo-osmolar conditions. Thereafter samples were treated with proteinase K (PK). In intact mitochondria, Mim2–HA is cleaved and a smaller fragment of about 11 kDa was detected (Fig. 1D, second lane). This fragment was not observed when the MOM was ruptured or when mitochondria were solubilized with detergent (Fig. 1D). The IMS localized protein Dld1 and the matrix protein Mge1 served to control the integrity of the outer and inner membranes,

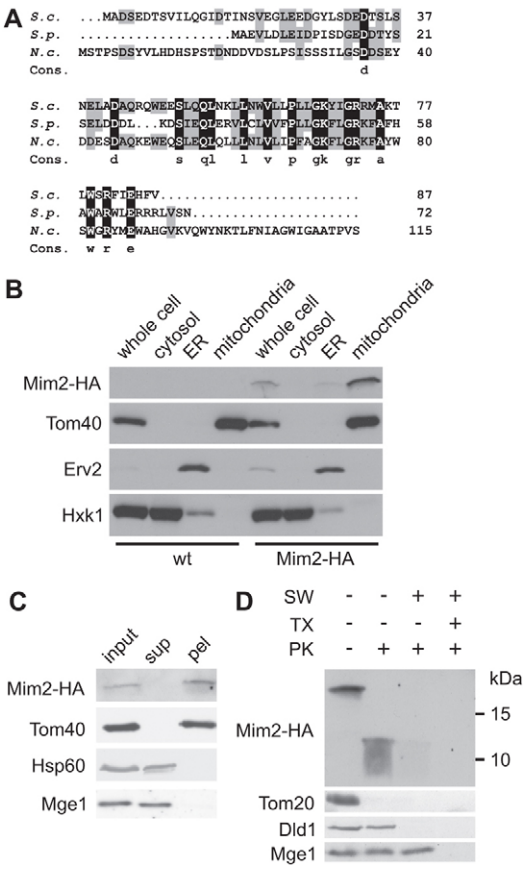

Fig. 1. Mim2 is an integral protein of the MOM with its C-terminus facing the intermembrane space. (**A**) Mim2 is conserved among fungi. Amino acid sequences of Mim2 from *Saccharomyces cerevisiae* (*S.c.*), *Schizosaccharomyces pombe* (*S.p.*) and *Neurospora crassa* (*N.c.*) are shown. Identical residues are depicted in white on black background, similar residues are highlighted in gray. (**B**) Mim2 is a mitochondrial protein. Whole-cell lysate (whole cell) and fractions corresponding to cytosol, light microsomal fraction (ER) and mitochondria of either wild-type cells or cells expressing Mim2–HA were analyzed by SDS-PAGE and immunodecoration with antibodies against the HA-tag, the mitochondrial protein Tom40, the ER protein Erv2 and a marker protein for the cytosol (hexokinase, Hxk1). (**C**) Mim2 is a membrane-embedded protein. Mitochondria isolated from cells expressing Mim2–HA were subjected to carbonate extraction. The supernatant (sup) and pellet (pel) fractions were analyzed by SDS-PAGE and immunodecoration with antibodies against the indicated proteins. Tom40, an integral OM protein; Hsp60 and Mge1, soluble matrix proteins. (**D**) The C-terminus of Mim2 is protected from protease digestion by the MOM. Mitochondria isolated from cells expressing Mim2–HA were treated with proteinase K (PK) under different conditions. Mitochondria were kept intact, the outer membrane was ruptured by hypo-osmolar swelling (SW) or mitochondria were lysed completely by the addition of the detergent Triton X-100 (TX). Samples were precipitated with trichloroacetic acid and analyzed by SDS-PAGE and immunodecoration with antibodies against the HA-tag, or the indicated mitochondrial proteins. Tom20, an OM protein exposed to the cytosol; Dld1, an IMS protein; Mge1, a matrix protein.

respectively. These results demonstrate that Mim2 is anchored in the MOM with its C-terminus facing the IMS.

An unusual feature of Mim2 is the distribution of charged amino acid residues along its sequence. Negatively charged residues cluster at the N-terminal region, whereas the C-terminal part is positively charged. While low concentrations of the

rather unspecific protease PK were sufficient to cleave Mim2–HA, treating intact mitochondria with high concentrations of trypsin, a protease cutting C-terminally to positively charged amino acids, did not result in a cleavage of Mim2–HA (supplementary material Fig. S3). These results further support our proposal that the positively charged C-terminal region of Mim2 is protected by the MOM. Taken together our findings suggest that Mim2 is an integral membrane protein of the MOM with its N-terminus located in the cytosol and the C-terminus residing in the IMS.

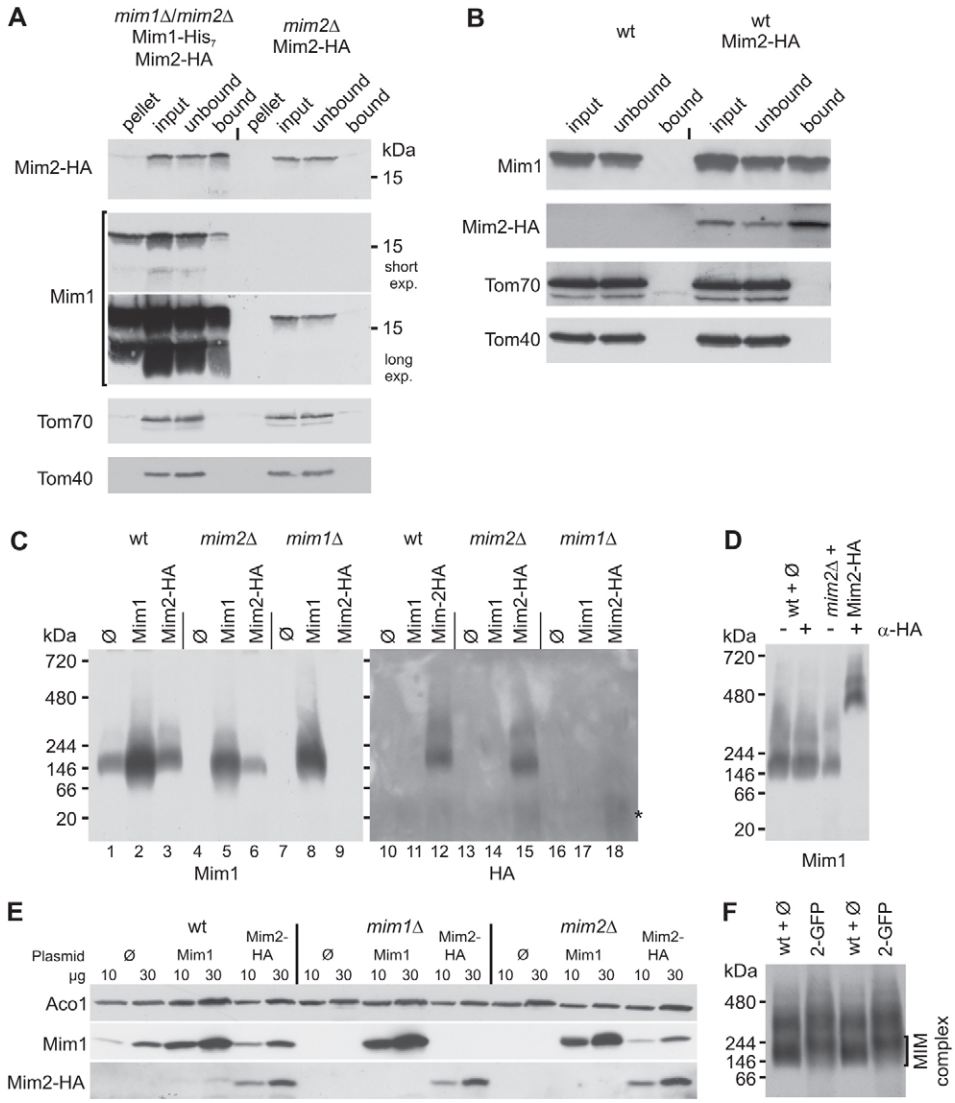

Fig. 2. Mim1 and Mim2 physically interact and are components of the same protein complex. (**A**) Mitochondria isolated from either the double-deletion strain *mim1*Δ/*mim2*Δ overexpressing Mim1-His$_7$ and Mim2–HA or a single deletion strain *mim2*Δ overexpressing Mim2–HA were employed. Organelles were lysed in digitonin-containing buffer and cleared supernatants were incubated with Ni–NTA beads. Non-solubilized matter (pellet), cleared supernatant (input, 20% of total), supernatant after binding to the beads (unbound, 20% of total) and material bound to the beads (bound, 100% of total) were analyzed by SDS-PAGE and immunodecoration with the indicated antibodies. (**B**) Mitochondria isolated from a strain overexpressing Mim2–HA (Mim2-HA) and the corresponding wild-type strain were lysed in digitonin-containing buffer. Cleared supernatants were incubated with ProteinG Sepharose beads preincubated with an antibody against the HA-tag. Supernatants before (input, 10% of total) and after (unbound, 10% of total) binding to the beads as well as bound material (bound, 100% of total) were analyzed by SDS-PAGE and immunodecoration with the indicated antibodies. (**C**) Mitochondria isolated from wild-type, *mim1*Δ or *mim2*Δ strains harboring an empty plasmid (Ø) or overexpressing either Mim1 or Mim2–HA were lysed in digitonin and analyzed by BN-PAGE. For analysis of Mim1 and Mim2–HA containing complexes, the membrane was immunodecorated with antibodies against Mim1 and the HA-tag, respectively. An unassembled species of Mim2–HA is indicated with an asterisk. (**D**) Mitochondria isolated from a wild-type or *mim2*Δ strains containing either empty plasmid (Ø) or overexpressing Mim2–HA were solubilized in digitonin, the lysate was cleared by centrifugation and then incubated with or without an antibody against the HA-tag (α-HA). Samples were analyzed by BN-PAGE and immunodecoration with an antibody against Mim1. (**E**) Two different amounts (10 μg and 30 μg) of the mitochondria described above in the legend to panel (C) were analyzed by SDS-PAGE and immunodecoration with the indicated antibodies. The matrix protein aconitase (Aco1) served as a control. (**F**) Mitochondria isolated from a wild-type strain containing empty plasmid (Ø) and a *mim2*Δ strain overexpressing GFP–Mim2 (2-GFP) were solubilized in digitonin, and samples were analyzed by BN-PAGE and immunodecoration with an antibody against Mim1. For easier observation of the small size difference, the same samples were loaded twice in alternating lanes. The MIM complex is indicated.

Mim1 and Mim2 physically interact and are components of the same complex

Although we identified Mim2 as a protein that associates with GFP–Mim1 we wanted to substantiate the interaction between the two proteins by additional pull-down experiments. Mitochondria were isolated from a *mim1*Δ/*mim2*Δ double-deletion strain overexpressing Mim1-His$_7$ (Popov-Celeketić et al., 2008) and Mim2–HA. A *mim2*Δ strain overexpressing Mim2–HA that contains non-tagged endogenous Mim1 served as a control (Fig. 2A). The isolated organelles were lysed and proteins were incubated with Ni–NTA beads to pull down Mim1-His$_7$. Subsequent SDS-PAGE and immunodecoration showed that Mim2–HA specifically bound to the affinity beads together with Mim1-His$_7$. No unspecific binding of Mim2–HA to the beads was observed with the control sample. Of note, the enrichment of Mim2–HA in the bound material was even higher than that of Mim1-His$_7$, suggesting a tight association of both proteins. A further potential explanation for this enrichment of Mim2 is that the binding of Mim2 to Mim1-His$_7$ causes a conformational change in the latter protein that in turn results in an increased accessibility of the His-tag for binding to the affinity beads.

To further verify this interaction, we performed the reciprocal co-immunoprecipitation experiment. Mitochondria isolated from a strain expressing Mim2–HA were solubilized with the mild detergent digitonin and then incubated with beads loaded with antibody specific for the HA-tag. A significant amount of the endogenous Mim1 was co-precipitated together with Mim2–HA (Fig. 2B). No unspecific binding of Mim1 to the beads was observed when the corresponding wild-type mitochondria were used as a control (Fig. 2B).

Mim1 was reported to be a component of a high molecular weight complex (Ishikawa et al., 2004; Waizenegger et al., 2005; Becker et al., 2008; Popov-Celeketić et al., 2008). Our results show that Mim1 and Mim2 tightly interact and indicate that Mim2 is a novel component of this Mim1-containing complex that we refer to as the MIM complex. To confirm this hypothesis, mitochondria from *mim1*Δ or *mim2*Δ strains overexpressing either Mim1 or Mim2–HA were analyzed by blue native gel electrophoresis (BN-PAGE). Both Mim1 and Mim2-HA migrated as a complex of approximately 200 kDa (Fig. 2C, compare lanes 3 and 12 and supplementary material Fig. S4) confirming that the two proteins are indeed components of the same oligomeric structure. Expression of Mim2–HA in the strain lacking endogenous Mim2 only partially restored the levels of the MIM complex as assessed by BN-PAGE (Fig. 2C, compare lane 6 to lane 1) although the steady-state levels of Mim1 as monitored by SDS-PAGE were almost normal (Fig. 2E). These observations suggest that even though Mim2–HA complements the *mim2*Δ growth phenotype, the HA-tag might interfere with the optimal interaction of Mim2 with Mim1.

Next, we investigated the importance of Mim2 and Mim1 for the formation of the MIM complex. Of note, no Mim1-containing oligomeric species could be detected in the absence of Mim2 and the protein could not be detected in SDS-PAGE and immunodecoration (Fig. 2C, lane 4; 2E). Hence, Mim2 is a crucial player in the biogenesis of Mim1 and the MIM complex. The absence of Mim1 has different effects as it leads to a loss of a detectable Mim2–HA-containing complex but unassembled species of the protein is present (Fig. 2C, lane 18; supplementary material Fig. S5) and expression levels of the protein are unaffected (Fig. 2E).

To further substantiate the participation of both proteins in the same complex we used mitochondria isolated from wild-type and *mim2*Δ cells transformed with either Mim2–HA encoding vector or an empty plasmid as control. Next we lysed the organelles with detergent and performed an antibody-shift assay where antibodies against the HA-tag were added to the lysed organelles before their analysis by BN-PAGE. The antibodies caused a shift in the migration of the Mim1 signal (Fig. 2D), suggesting that both Mim1 and Mim2 are subunits of the same MIM complex.

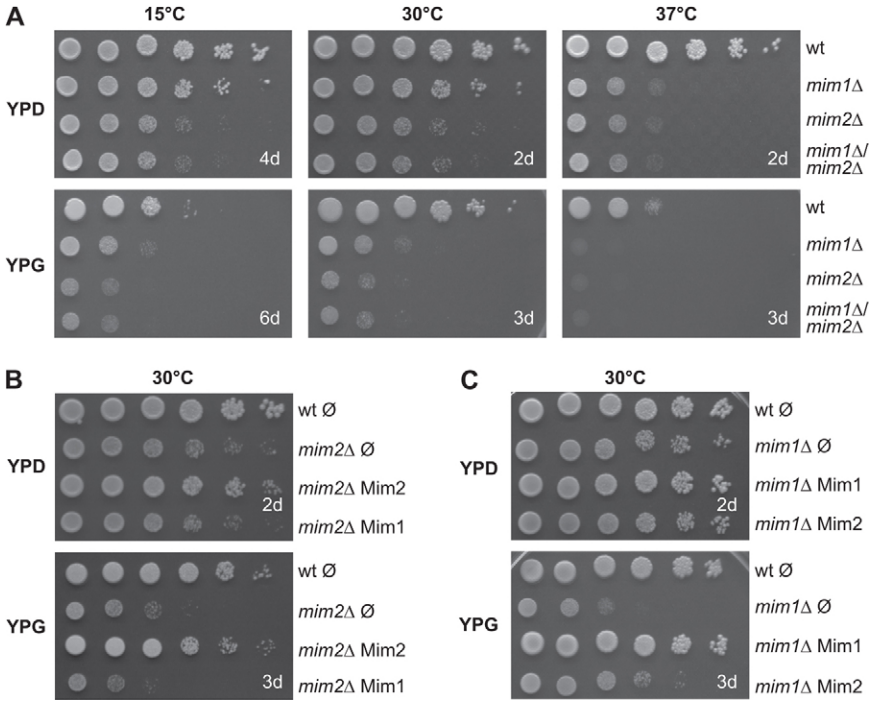

Fig. 3. Deletion of *MIM2* results in severe growth phenotypes. (**A**) Cells that lack Mim1, Mim2 or both proteins show reduced growth at all conditions. The indicated strains were tested at three different temperatures by drop-dilution assay for growth on rich medium containing the fermentable carbon source glucose (YPD) or the non-fermentable carbon source glycerol (YPG). Pictures were taken after the indicated number of days. (**B**) Overexpression of Mim1 does not rescue the growth defect of a *mim2*Δ strain. Wild-type cells transformed with an empty plasmid and *mim2*Δ cells transformed with an empty plasmid, Mim2 encoding plasmid or Mim1 encoding plasmid were analyzed by drop-dilution assay on YPD or YPG medium. (**C**) Overexpression of plasmid-borne Mim2 partially rescues the growth defect of the *mim1*Δ strain. Wild-type cells transformed with an empty plasmid and *mim1*Δ cells transformed with an empty plasmid, Mim1 encoding plasmid, or Mim2 encoding plasmid were analyzed by drop-dilution assay on YPD or YPG medium.

Of note, overexpression of Mim1 in the absence of Mim2 resulted in a complex with apparent similar migration behavior to the native complex (Fig. 2C, compare lane 1 to 5). Hence, it seems that Mim2 is not absolutely required for the formation of Mim1-containing complex. This observation further suggests that the native MIM complex probably contains only one or two copies of Mim2. Therefore the absence of Mim2 causes only a minor difference of 10–20 kDa in the mass of the MIM complex and such a difference in turn is hard to resolve by BN-PAGE. In order to obtain further support for our assumption that the two proteins are components of the same native complex, we analyzed the MIM complex in organelles harbouring GFP-tagged Mim2. If Mim1 is a component in the same complex as Mim2, the additional mass of the GFP moiety should shift also the band of the Mim1-containing complex as analyzed by BN-PAGE. Indeed, clear slower migration behavior of the Mim1-complex was observed in the organelles harboring the GFP-tagged Mim2 (Fig. 2F). Taken together, our results suggest that Mim1 and Mim2 are components of the same protein complex.

Deletion of MIM2 causes severe growth phenotype

The ORF *YLR099W-A/MIM2* was reported in a systematic deletion attempt to be an essential gene (Kastenmayer et al., 2006). We wanted to confirm the reported lethality by deleting the complete ORF of *MIM2* in the diploid yeast strain W303a/α and then performing tetrad analysis. After sporulation and tetrad dissection, haploid *mim2*Δ strains were retrieved as confirmed by PCR (data not shown). In contrast to the reported lethality, this deletion strain was viable although it showed a severe growth reduction on fermentable and non-fermentable carbon sources at all tested temperatures (Fig. 3A). The growth behavior of the *mim2*Δ strain is even worse than that of the strain lacking Mim1 and the double-deletion strain grows like the *mim2*Δ strain (Fig. 3A). To exclude the possibility that the observed phenotypes were caused by unrelated changes, e.g. changes in the promoter region of the essential *ERG27* gene – which is in close proximity on the chromosome to the *MIM2* gene – we aimed to complement these phenotypes by plasmid-encoded Mim2. Overexpression of native or the C-terminally tagged version of Mim2 could rescue the growth phenotype of the deletion mutant confirming that the observed phenotypes are related to the absence of the Mim2 protein (supplementary material Fig. S2).

MIM2 and MIM1 genetically interact

Our results suggest that Mim1 and Mim2 physically interact and are components of the same protein complex. Hence we asked whether the two ORFs also genetically interact. We could not observe a synthetic growth phenotype by deletion of both genes (Fig. 3A). Of note, overexpression of Mim1 in yeast cells lacking Mim2 slightly hampered the growth of the *mim2*Δ strain (Fig. 3B). Accordingly, the steady-state levels of the MIM substrate Ugo1 are somewhat reduced in these cells (supplementary material Fig. S6). On the other hand, overexpression of Mim2 in a *mim1*Δ strain led to partial rescue of the growth phenotype (Fig. 3C). This partial rescue was observed in six independent transformants and was paralleled by elevated levels of Ugo1. Furthermore, the overexpression of Mim2–HA in the *mim1*Δ strain caused higher levels of Tom40 and less unassembled Tom40 molecules as compared to *mim1*Δ cells (supplementary material Fig. S7). These results suggest that higher levels of Mim2 can reduce the dependency on Mim1 for some processes. Collectively, in addition to their physical association, *MIM1* and *MIM2* genetically interact.

Deletion of MIM2 leads to abnormal mitochondrial morphology

It was previously reported that downregulation of Mim1 leads to altered mitochondrial morphology (Altmann and Westermann, 2005; Dimmer and Rapaport, 2010). It is assumed that this phenotype results from the impaired assembly of the TOM complex and the subsequent insufficient import of morphology

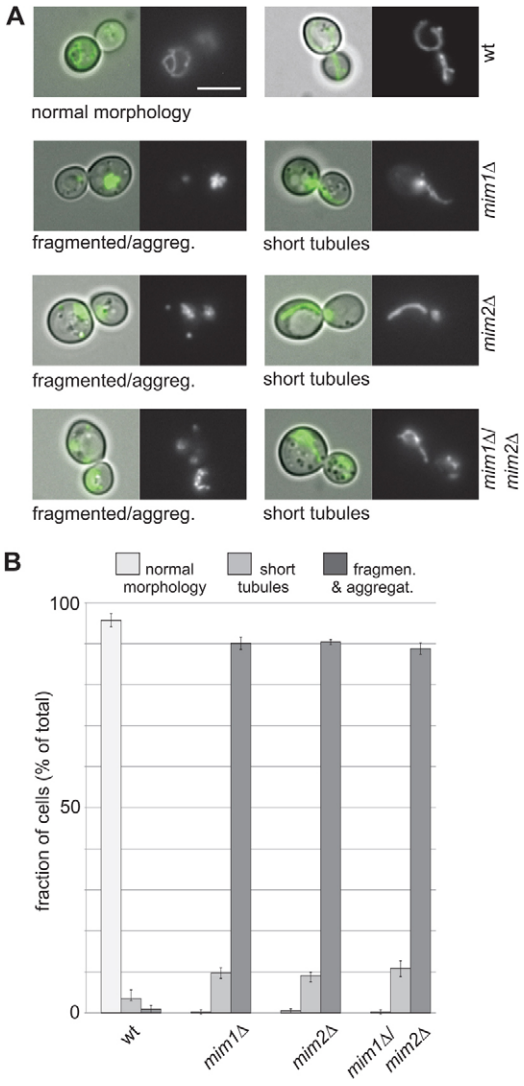

Fig. 4. Cells that lack Mim1, Mim2 or both proteins show altered mitochondrial morphology. (**A**) Cells of the indicated strains transformed with mitochondrially targeted GFP (pSu9-GFP) were analyzed by fluorescence microscopy. Examples of predominant phenotypes (fragmented/aggregated and short tubular) for each strain are shown (scale bar: 5 μm). (**B**) Analyzed cells of the various strains were grouped into three different morphology phenotypes (normal, short tubules, and fragmented and aggregated). Statistical analysis of four different experiments, in which ⩾100 cells per experiment were analyzed, was performed and the various occurrences of the phenotypes are presented.

relevant proteins. We verified this phenotype by deletion of *MIM1* in the wild-type background W303 (Fig. 4A). Typically for this deletion strain, mitochondria were fragmented and aggregated in approximately 90% of the cells (Fig. 4B). Very similar morphological phenotype was observed upon deletion of *MIM2* alone or in the *mim1*Δ/*mim2*Δ double-deletion strain (Fig. 4A,B). These results provide further evidence that Mim1 and Mim2 function in the same molecular pathway.

Loss of Mim2 leads to reduced biogenesis of mitochondrial proteins

To gain further insight into the function of Mim2, we analyzed the steady-state levels of proteins in mitochondria isolated from *mim2*Δ cells. Of note, Mim1 was hardly detectable in these organelles and a severe reduction was observed in the levels of the MOM proteins Tom20, Fzo1 and Ugo1 – known substrates of Mim1 (Fig. 2E; Fig. 5A, left panel) (Waizenegger et al., 2005; Becker et al., 2011; Papic et al., 2011). In contrast to Tom20, the levels of all other TOM components tested – Tom40, Tom22 and Tom70 – did not show a significant reduction in mitochondria lacking Mim2. Similarly, the steady-state levels of other mitochondrial proteins like the MOM β-barrel protein Por1, the tail-anchored protein Fis1, the inner membrane proteins Oxa1 and Dld1, as well as the matrix proteins Hsp60 and aconitase were unaltered in comparison to those in wild-type organelles (Fig. 5A, right panel).

We next compared the assembly status of the TOM complex in mitochondria isolated from strains lacking Mim2, Mim1 or both. The amount of assembled TOM complex as assessed by immunodecoration with antibodies against Tom40 and Tom22 was drastically reduced when *MIM1*, *MIM2* or both were deleted (Fig. 5B). Concomitantly, an unassembled species of Tom40 was observed in the mutated cells. The observations regarding the reduced stability of the TOM complex in *mim1*Δ cells are in line with previous reports (Ishikawa et al., 2004; Waizenegger et al., 2005). The assembly of the TOB complex as monitored by BN-PAGE was unchanged in these deletion strains (Fig. 5B). Collectively, the absence of Mim2 resulted in reduced steady-state levels of Tom20 and multispan MOM proteins as well as reduced stability of the TOM complex.

Mitochondria lacking Mim2 show compromised import of multispan MOM proteins

Since the steady-state levels of certain mitochondrial proteins were reduced in mitochondria lacking Mim2, we investigated its role in mitochondrial protein import. To this end we first analyzed whole-cell extracts for accumulation of mitochondrial precursor proteins, a phenotype that was observed in cells lacking Mim1 (Ishikawa et al., 2004; Mnaimneh et al., 2004; Waizenegger et al., 2005). We observed a clear accumulation of unprocessed precursor form of the matrix protein Hep1 in extracts from cells lacking Mim1 or Mim2 or both proteins (Fig. 6A). This indicates a global import defect of mitochondria lacking Mim2.

Next we investigated the in vitro import for model substrates located in the different mitochondrial compartments. Isolated mitochondria were incubated with radioactive precursor proteins for different time points and import was assessed by SDS-PAGE and autoradiography. The import efficiencies for the matrix destined preprotein pSu9-DHFR, the inner membrane protein AAC, as well as the β-barrel precursor porin were reduced (Fig. 6B). Of note, the most pronounced reduction was in the case of the MOM multispan proteins Ugo1 and Fzo1 (Fig. 6B). In

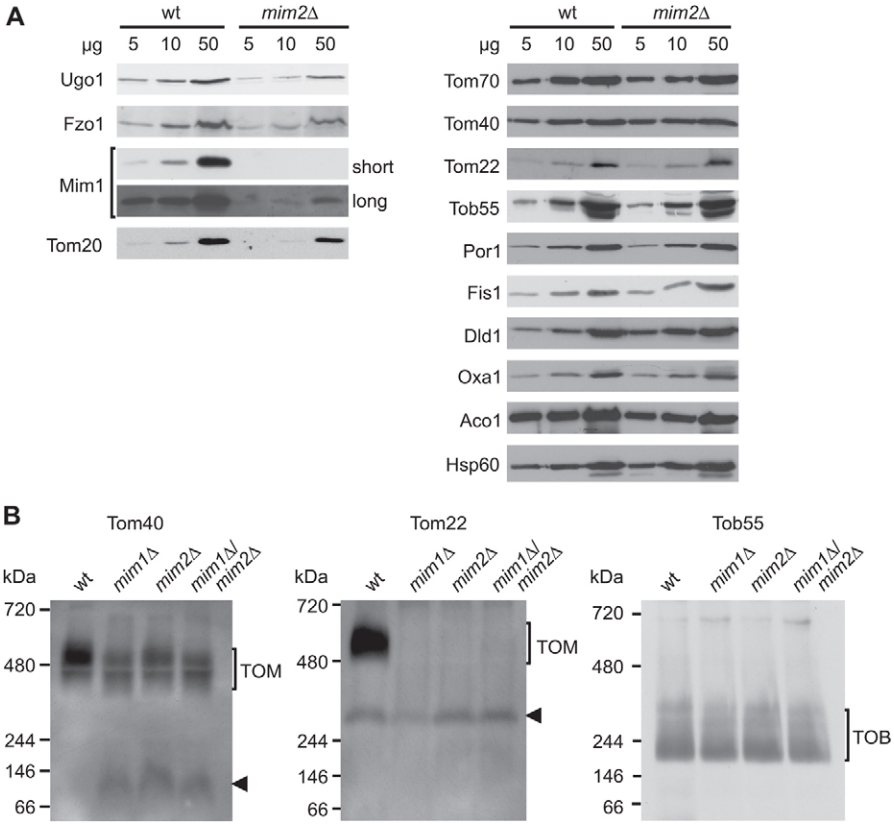

Fig. 5. Absence of Mim2 leads to reduced steady-state levels of helical MOM proteins and a compromised assembly of the TOM complex. (**A**) Various amounts of mitochondria (5, 10 and 50 µg) isolated from wild-type and *mim2*Δ cells were analyzed by SDS-PAGE and immunodecoration with the indicated antibodies. A representative experiment of three different independent repeats is presented. (**B**) Mitochondria of the indicated strains were first lysed in 1% digitonin (for TOM analysis) or in 0.5% Triton X-100 (for TOB analysis) and then subjected to BN-PAGE and immunoblotting with the indicated antibodies. Arrowheads indicate the Tom40-containing low molecular mass species and the Tom22 assembly intermediate. The assembled TOM and TOB complexes are indicated. A representative experiment of three different independent repeats is presented.

contrast, the import of the tail-anchored MOM protein Fis1, which is inserted independently of any known import factors (Kemper et al., 2008), was unaffected by the absence of Mim2 (data not shown). The global defect in mitochondrial import results most probably from a reduced number of functional TOM complexes. In accordance with the reduced steady-state levels of assembled TOM complex in mitochondria lacking Mim2 (Fig. 5B), the assembly of newly synthesized Tom40 molecules into the TOM complex is severely hampered in *mim2*Δ cells (Fig. 6C).

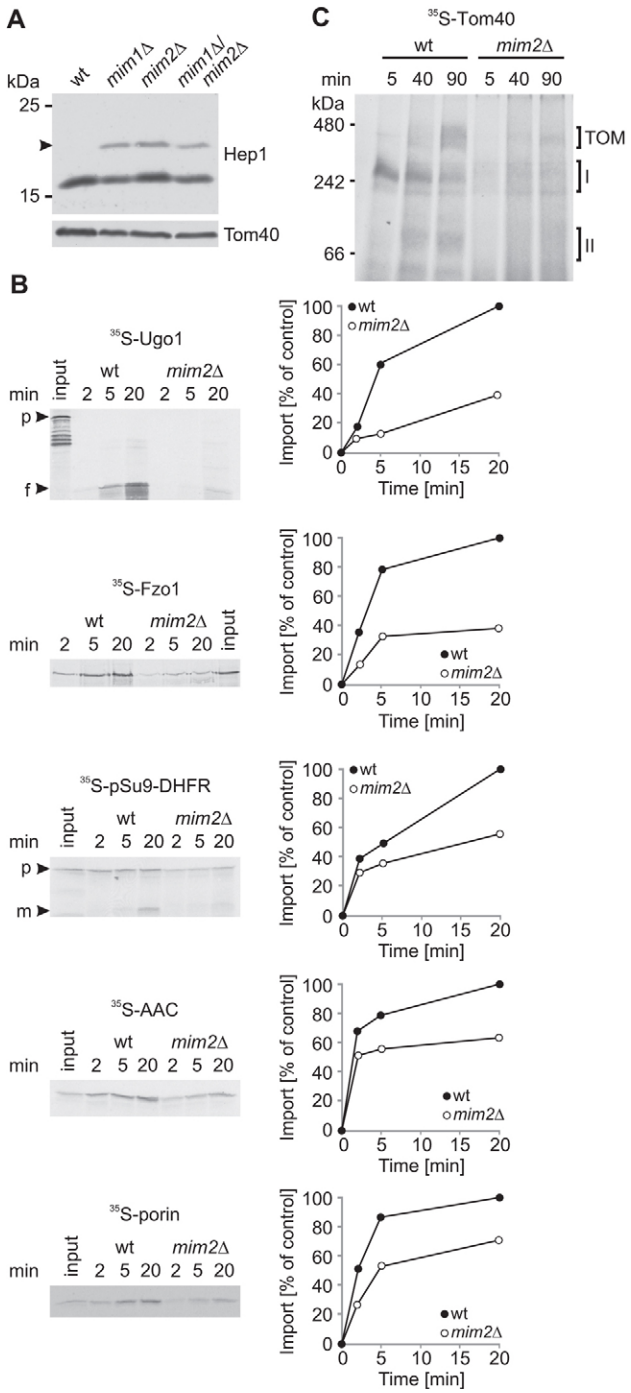

We aimed to analyze the direct import defects due to lower levels of Mim2 avoiding the global outcome resulting from compromised biogenesis of Tom components and hampered assembly of the TOM complex. To that end a yeast strain in which the expression of *MIM2–HA* was under the control of the *GAL1* promoter was constructed. In the presence of galactose the cells grew like wild-type cells whereas growth on glucose was strongly compromised. We first tested the levels of various mitochondrial proteins in total cell lysates from the *GAL1–MIM2–HA* cells grown at various time periods after the shift from galactose- to glucose-containing medium (data not shown). On the basis of this analysis we isolated mitochondria from cells grown for 15 h on glucose and analyzed their proteins by immunodecoration. Of note, Mim2 and its partner protein Mim1 were hardly detectable in these organelles whereas the Tom components were still in normal levels (supplementary material Fig. S8A). Furthermore, the TOM complex as analyzed by BN-PAGE was also detected in normal levels (supplementary material Fig. S8B). Next, in vitro import assays were performed with mitochondria depleted for Mim2. Importantly, whereas the insertion of the MIM substrate Ugo1 into these organelles was compromised, no import defects were observed for the TOM substrates pSu9-DHFR and porin (supplementary material Fig. S8C). Taken together the results suggest that the absence of Mim2 causes two effects: a specific reduction in membrane integration of some outer membrane helical proteins and subsequently a global import defect due to altered stability of the TOM complex.

Mim2 is directly involved in the import of Ugo1

Finally, we asked whether Mim2 actually participates in interactions with substrate proteins. To that end, we analyzed import reactions of newly synthesized [^{35}S]Ugo1 by BN-PAGE in combination with an antibody-shift assay. Mitochondria were isolated from wild-type and *mim2*Δ cells transformed with an empty plasmid and a plasmid encoding Mim2–HA, respectively. After import of Ugo1, mitochondria were lysed in digitonin,

Fig. 6. Deletion of *MIM2* leads to various import defects and impaired assembly of the TOM complex. (**A**) Whole-cell lysates of wild type cells and those lacking Mim1, Mim2 or both proteins were analyzed by SDS-PAGE and immunodecoration with the indicated antibodies. The precursor of the mitochondrial matrix protein Hep1 is indicated by an arrowhead. (**B**) Mitochondria isolated from a wild-type or *mim2*Δ strain were incubated with the indicated radiolabeled precursor proteins for the indicated time periods. At the end of the import reactions samples were treated as described below, analyzed by SDS-PAGE and autoradiography, and bands corresponding to imported material were quantified. Samples containing radiolabeled Ugo1 were trypsinated in order to generate a specific 23 kDa fragment (f) (see Papic et al., 2011). After import of Fzo1, carbonate extraction was performed and the membranous fraction was analyzed; when pSu9-DHFR was imported, the mature protein (m) was quantified. After import of porin and AAC mitochondria were treated with PK and the protected molecules were quantified. The intensity of bands representing imported material into wild-type mitochondria for the longest time period was set as 100%. (p) precursor form of pSu9-DHFR and full-length Ugo1. A representative experiment of three independent repeats is presented. (**C**) Radiolabeled precursor of Tom40 was imported into mitochondria that had been isolated from *mim2*Δ or the corresponding wild-type strain. After import, the mitochondria were solubilized with digitonin and analyzed by BN-PAGE and autoradiography. The two assembly intermediates of Tom40 (I, II) and the assembled TOM core complex (TOM) are indicated.

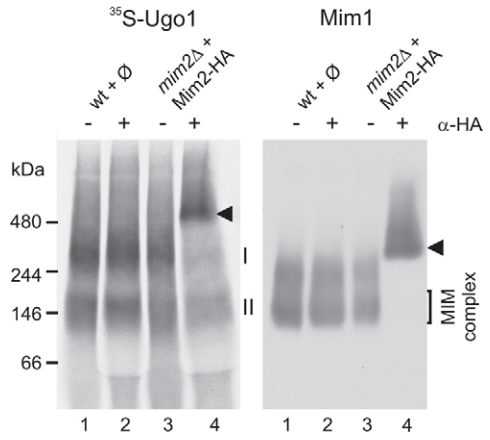

Fig. 7. Mim2 is directly involved in Ugo1 import. Mitochondria isolated from a wild-type strain containing the empty plasmid (Ø) and from a *mim2*Δ strain overexpressing Mim2–HA were incubated with radiolabeled precursor of Ugo1. After the import reactions mitochondria were solubilized in digitonin; the lysate was cleared by centrifugation and then incubated with or without an antibody against the HA-tag (α-HA). Samples were analyzed by BN-PAGE, autoradiography (left panel) and then immunodecoration with an antibody against Mim1 (right panel). Mim2-containing complexes that were shifted by the antibody are indicated by an arrowhead.

halved and an antibody specific for the HA-tag was added to one portion. Strikingly, addition of the antibody resulted in a shift of the radioactive signal of [^{35}S]Ugo1 to higher molecular weights only if mitochondria harboring Mim2–HA were used (Fig. 7, left panel, arrowhead). Thus, Mim2 interacts with substrate proteins. A similar shift was observed for the Mim1 signal (Fig. 7, right panel) suggesting that both Mim1 and Mim2 are subunits of the functional substrate-binding MIM complex.

Taken together, this study reveals that the integral MOM protein Mim2 is a novel component of the MIM complex that mediates the import of integral MOM helical proteins.

Discussion

In this work we report on the identification of Mim2 as a novel protein with a crucial function in the biogenesis of mitochondria. Mim2 is located in the MOM, exposing its N-terminus to the cytosol and the C-terminus to the IMS. The protein shares this topology with its binding partner Mim1 and it also shows functional similarity to the latter protein. Altered mitochondrial morphology, reduced growth, lower steady-state levels of several mitochondrial components as well as compromised assembly of TOM complex are consequences of both *MIM2* and *MIM1* deletion. Mim1, Tom20 and the multispan proteins of the MOM seem to be the main substrates that are affected by the absence of Mim2. We propose that hampered biogenesis in the absence of Mim2 results in reduced steady-state amounts and assembly of different proteins in *mim2*Δ cells that in turn cause the other observed phenotypes in these cells. For example, the altered morphology of mitochondria in *mim1*Δ and *mim2*Δ cells can be explained by the lower levels of their substrate proteins Fzo1 and Ugo1. The latter two proteins mediate mitochondrial fusion and thus their reduced levels interfere with the balance between fusion and fission of the organelles.

Strikingly, the steady-state level of Mim1 is severely reduced in mitochondria lacking Mim2. This finding might suggest that the observed effects in *mim2*Δ cells are solely due to the loss of Mim1. Yet several observations are in contrast to this scenario. First, the growth phenotype of *mim1*Δ cells can be partially rescued by the overexpression of Mim2. Therefore additional copies of Mim2 can, to a certain extent, reduce the requirement for Mim1. Second, overexpression of Mim1 in a *mim2*Δ strain does not improve the growth retardation but rather has even somewhat negative effect on growth. These observations suggest a unique function of Mim2 and might indicate that in the absence of Mim2 some unassembled Mim1 molecules exert a dominant-negative effect by competing with the function of the MIM complex. Third, our pull-down experiments and native electrophoresis assays demonstrate that both proteins are present in a stable functional complex that interacts with substrate proteins.

Our results shed new light on the stoichiometry of the MIM complex as they show that reduced levels of Mim1 or its overexpression have a minor effect on complex size. Thus it seems that the actual complex of around 200 kDa contains a rather fixed number of copies of Mim1 and Mim2. In the absence of Mim1 we could not observe a Mim2-containing sub-complex suggesting that Mim1 is a crucial component for the formation of the MIM complex. In contrast, a Mim1-containing complex was formed even in the absence of Mim2 suggesting that the latter protein is not absolutely essential for complex formation. Naturally, we cannot exclude the possibility that additional, yet to be identified, proteins are further components of the MIM complex. Future efforts to functionally reconstitute the complex from isolated subunits can provide an answer to this open question. Taken together, the identification and characterization of Mim2 get us one step ahead in solving the riddle of import of outer membrane proteins, yet the elucidation of the precise composition of the MIM complex and its molecular mode of action has to be the next venture.

Materials and Methods

SILAC-based immunoprecipitation

*Mim1*Δ (YPH499 background) cells expressing plasmid encoding either native Mim1 or GFP-Mim1 were grown in synthetic media containing either $^{15}N_2$-$^{13}C_6$ lysine (heavy) or (light) lysine (Ong et al., 2002). Cells were harvested in mid-exponential phase and mitochondria were isolated after enzymatic spheroblastation, using an abridged protocol. EDTA was omitted from all buffers. Mitochondria were lysed in 1% digitonin, 10% (v/v) glycerol, 150 mM NaCl, 50 mM MOPS/KOH, pH 7.4, containing complete protease inhibitor cocktail (Roche). Samples were clarified by centrifugation and incubated with GFP-binder beads (gta100, Chromotek). Beads were isolated, washed and pooled according to forward (Mim1 light and GFP–Mim1 heavy) and reverse (Mim1 heavy and GFP–Mim1 light) experiments. Proteins were eluted with 4% SDS, 100 mM Tris–HCl pH 8.0, 0.1 M DTT and subjected to filter aided sample preparation method and digestion with endoproteinase (Wiśniewski et al., 2009).

Mass spectrometry and data analysis

Peptides were separated by nLC at 4 h gradient length without prior fractionation, electrosprayed online and analyzed with LTQ-Orbitrap-XL or Orbitrap-Velos mass spectrometers using collision-induced dissociation or higher-energy collisional dissociation fragmentation, respectively (Olsen et al., 2005; Olsen et al., 2009). Data analysis was performed using the MaxQuant software environment (Cox and Mann, 2008) version 1.0.13.9. Searches of generated peak lists were carried out with Mascot (Perkins et al., 1999) against the translation of all 6809 gene models from the Saccharomyces Genome Database (release date 12 December 2007) and 175 frequently observed contaminants. Identifications were accepted at a false discovery rate of 1% both at the peptide and protein level using a decoy database strategy with reversed protein sequences (Elias and Gygi, 2007).

Yeast strains and growth conditions

Standard genetic techniques were used for growth and manipulation of yeast strains. Unless otherwise stated, the wild-type strain W303 was used. The *mim1*Δ/*mim2*Δ double-deletion strain was obtained by mating of the single deletion strains followed by tetrad dissection. Transformation of yeast was carried out according to the

lithium-acetate method. For drop-dilution assays, yeast cells were grown in synthetic medium to an OD_{600} of 1.0, diluted in fivefold increment, and then 5 µl of each dilution were spotted onto solid media and growth was monitored for few days.

Recombinant DNA techniques

To express Mim1 or Mim2 in yeast cells with or without a C-terminal HA-tag, the ORF of *MIM1* or *MIM2* (systematic name *YHR099W-A*) was amplified by PCR with or without its stop codon using yeast genomic DNA as template. Primers used contained *Eco*RI and *Hind*III restriction sites which were used to introduce the amplified fragment into the expression vector pYX142 which contains the HA-tag sequence. Constructs were verified by sequencing. For expression of Mim1 with a C-terminal His_7-tag, the plasmid pRS426-TPIpro-Mim1-His_7 was used (Popov-Celeketić et al., 2008).

Yeast genes were deleted by a PCR-based approach using the HIS3 marker amplified from pFA6a-His3MX6 plasmid (Wach et al., 1997) or the kanamycin resistance cassette amplified from pFA6a-kanMX4 plamid (Wach et al., 1994). For the deletion of *MIM1* the primers KSD311 (5′-AGAAACATCACCCCCTTCT-TACGAAACTGCCACAAGACAGAAATCGTACGCTGCAGGTCGAC-3′) and KSD 312 (5′-GTGTGTGTATTTATTTATGTAGGTTGCTAATGCTTTGGTGAT-CGTATCGATGAATTCGAGCTCG-3′) were used, for MIM2 KSD099f (5′-CCCAGCACCACAGCACATCACTGCACGAGCAACAATAACTAGAACCGT-ACGCTGCAGGTCGAC-3′) and KSD099r (5′-TTATCTGTTATAACTGCTA-TATGCGGATACATAAACAACAAACACATCGATGAATTCGAGCTCG-3′). Deletion of genes was confirmed by screening-PCR. Haploid deletions strains were obtained by tetrad dissection.

A yeast strain harboring Mim2 under the control of an inducible promoter was obtained by transforming the pYX113-GAL1pro-*MIM2*-HA vector into *mim2*Δ strain. To construct this plasmid the *MIM2* ORF without the stop codon was subcloned from pYX142-*MIM2*-HA. For expression of GFP–Mim2 the ORF of *MIM2* was cloned into pYX132-Nterm-GFP using *BamH*I and *Hind*III sites. The pYX132-Nterm-GFP plasmid contains the coding sequence for GFP without a stop codon cloned between *Eco*RI and *BamH*I sites.

Biochemical procedures

Mitochondria were isolated from yeast cells by differential centrifugation as previously described (Daum et al., 1982). Subcellular fractionation was performed according to published procedures (Walther et al., 2009). Import experiments with radiolabeled precursor proteins and isolated mitochondria were performed in an import buffer containing 250 mM sucrose, 0.25 mg/ml BSA, 80 mM KC1, 5 mM $MgCl_2$, 10 mM MOPS–KOH, 2 mM NADH, 2 mM ATP, pH 7.2. Radiolabeled precursor proteins were synthesized in rabbit reticulocyte lysate in the presence of [^{35}S]methionine. Import assays for the mitochondrial precursor proteins pSu9-DHFR, AAC, Porin, and Ugo1 were performed as described before (Papic et al., 2011). For swelling experiments, isolated mitochondria were incubated with a hypotonic buffer (20 mM HEPES, pH 7.2) for 30 min on ice. In the carbonate extraction reaction mitochondria were dissolved in 0.1 M Na_2CO_3. After 30 min on ice, samples were centrifuged (75,000 ***g***, 60 min, 2℃) and pellet and supernatant were analyzed.

For pull-down experiments, mitochondria from the *mim1*Δ/*mim2*Δ yeast strain expressing Mim2–HA and Mim1-His_7 or the *mim2*Δ strain expressing Mim2–HA were used. After lysis in digitonin buffer (0.5% digitonin, 20 mM Tris-HCl, 50 mM NaCl, 10% glycerol, 1 mM PMSF, pH 7.4) and clarifying spin (20,000 ***g***, 20 min, 2℃) supernatants were incubated for 1 h at 2℃ with Ni-NTA agarose beads (NEB) that were pre-equilibrated in digitonin-buffer. After washing twice, bound material was analyzed by SDS-PAGE and immunodecoration.

Co-immunoprecipitation experiments were performed using isolated wild-type mitochondria and mitochondria isolated from a strain expressing Mim2–HA. After binding of the HA-antibody to Protein G Sepharose beads these were incubated with cleared lysate of the mitochondria in digitonin buffer (1% digitonin, 20 mM Tris–HCl, 50 mM NaCl, 10% glycerol, 1 mM PMSF, pH 7.4). After several washes, bound proteins were analyzed by SDS-PAGE and immunodecoration.

Protein samples were analyzed by SDS-PAGE and blotting to nitrocellulose membranes followed by visualization through autoradiography. Alternatively, incubation with antibodies was carried out according to standard procedures and visualization was performed via the ECL method. Intensity of the observed bands was quantified with the AIDA software (Raytest). Unless stated otherwise, each presented experiment represents at least three independent repetitions.

Blue native PAGE

Mitochondria were lysed in 40 µl TX-100 or digitonin buffer (0.5% TX-100 or 1-1.5% digitonin, 20 mM Tris-HCl, 0.1 mM EDTA, 50 mM NaCl, 10% glycerol, 1 mM PMSF, pH 7.4). After incubation for 15 min at 4℃ and a clarifying spin (30000 ***g***, 15 min, 2℃), 5 µl sample buffer (5% [w/v] Coomassie Brilliant Blue G-250, 100 mM Bis-Tris, 500 mM 6-aminocaproic acid, pH 7.0) were added, and the mixture was analyzed by electrophoresis in a 6 to 13% gradient blue native gel (Schägger et al., 1994). Gels were blotted to polyvinylidene fluoride membranes and proteins were further analyzed by autoradiography or immunodecoration. For antibody shift, the antibody was added to the cleared mitochondrial lysate and the samples were incubated 30 min on ice prior to the addition of the sample buffer.

Fluorescence microscopy

For visualization of mitochondria, cells were transformed with a yeast expression vector harboring the mitochondrial presequence of subunit 9 of the F_o-ATPase of *N. crassa* fused to GFP, pVT100U-mtGFP (Westermann and Neupert, 2000). Microscopy images were acquired with an Axioskop20 fluorescence microscope equipped with an Axiocam MRm camera using the 43 Cy3 filter set and the AxioVision software (Zeiss).

Acknowledgements

We thank K. Rehn and E. Kracker for technical support, F. Essmann for helpful discussions and critically reading the manuscript, and J. Müller (IFIB, Tübingen, Germany) and A. Barna (IFIB, Tübingen, Germany) for providing plasmids.

Funding

This work was supported by the Deutsche Forschungsgemeinschaft [grant number RA 1048/4-1 to D.R.], and a postdoctoral fellowship from the Carl Zeiss Stiftung (K.S.D.).

Supplementary material available online at
http://jcs.biologists.org/lookup/suppl/doi:10.1242/jcs.103804/-/DC1

References

Ahting, U., Waizenegger, T., Neupert, W. and Rapaport, D. (2005). Signal-anchored proteins follow a unique insertion pathway into the outer membrane of mitochondria. *J. Biol. Chem.* **280**, 48-53.

Altmann, K. and Westermann, B. (2005). Role of essential genes in mitochondrial morphogenesis in Saccharomyces cerevisiae. *Mol. Biol. Cell* **16**, 5410-5417.

Becker, T., Pfannschmidt, S., Guiard, B., Stojanovski, D., Milenkovic, D., Kutik, S., Pfanner, N., Meisinger, C. and Wiedemann, N. (2008). Biogenesis of the mitochondrial TOM complex: Mim1 promotes insertion and assembly of signal-anchored receptors. *J. Biol. Chem.* **283**, 120-127.

Becker, T., Guiard, B., Thornton, N., Zufall, N., Stroud, D. A., Wiedemann, N. and Pfanner, N. (2010). Assembly of the mitochondrial protein import channel: role of Tom5 in two-stage interaction of Tom40 with the SAM complex. *Mol. Biol. Cell* **21**, 3106-3113.

Becker, T., Wenz, L. S., Krüger, V., Lehmann, W., Müller, J. M., Goroncy, L., Zufall, N., Lithgow, T., Guiard, B., Chacinska, A. et al. (2011). The mitochondrial import protein Mim1 promotes biogenesis of multispanning outer membrane proteins. *J. Cell Biol.* **194**, 387-395.

Burri, L., Vascotto, K., Gentle, I. E., Chan, N. C., Beilharz, T., Stapleton, D. I., Ramage, L. and Lithgow, T. (2006). Integral membrane proteins in the mitochondrial outer membrane of Saccharomyces cerevisiae. *FEBS J.* **273**, 1507-1515.

Chacinska, A., Koehler, C. M., Milenkovic, D., Lithgow, T. and Pfanner, N. (2009). Importing mitochondrial proteins: machineries and mechanisms. *Cell* **138**, 628-644.

Cox, J. and Mann, M. (2008). MaxQuant enables high peptide identification rates, individualized p.p.b.-range mass accuracies and proteome-wide protein quantification. *Nat. Biotechnol.* **26**, 1367-1372.

Daum, G., Gasser, S. M. and Schatz, G. (1982). Import of proteins into mitochondria. Energy-dependent, two-step processing of the intermembrane space enzyme cytochrome b2 by isolated yeast mitochondria. *J. Biol. Chem.* **257**, 13075-13080.

Dimmer, K. S. and Rapaport, D. (2010). The enigmatic role of Mim1 in mitochondrial biogenesis. *Eur. J. Cell Biol.* **89**, 212-215.

Dukanovic, J. and Rapaport, D. (2011). Multiple pathways in the integration of proteins into the mitochondrial outer membrane. *Biochim. Biophys. Acta* **1808**, 971-980.

Elias, J. E. and Gygi, S. P. (2007). Target-decoy search strategy for increased confidence in large-scale protein identifications by mass spectrometry. *Nat. Methods* **4**, 207-214.

Endo, T. and Yamano, K. (2009). Multiple pathways for mitochondrial protein traffic. *Biol. Chem.* **390**, 723-730.

Hubner, N. C., Bird, A. W., Cox, J., Splettstoesser, B., Bandilla, P., Poser, I., Hyman, A. and Mann, M. (2010). Quantitative proteomics combined with BAC TransgeneOmics reveals in vivo protein interactions. *J. Cell Biol.* **189**, 739-754.

Hulett, J. M., Lueder, F., Chan, N. C., Perry, A. J., Wolynec, P., Likić, V. A., Gooley, P. R. and Lithgow, T. (2008). The transmembrane segment of Tom20 is recognized by Mim1 for docking to the mitochondrial TOM complex. *J. Mol. Biol.* **376**, 694-704.

Ishikawa, D., Yamamoto, H., Tamura, Y., Moritoh, K. and Endo, T. (2004). Two novel proteins in the mitochondrial outer membrane mediate beta-barrel protein assembly. *J. Cell Biol.* **166**, 621-627.

Kastenmayer, J. P., Ni, L., Chu, A., Kitchen, L. E., Au, W. C., Yang, H., Carter, C. D., Wheeler, D., Davis, R. W., Boeke, J. D. et al. (2006). Functional genomics of

genes with small open reading frames (sORFs) in S. cerevisiae. *Genome Res.* **16**, 365-373.

Kemper, C., Habib, S. J., Engl, G., Heckmeyer, P., Dimmer, K. S. and Rapaport, D. (2008). Integration of tail-anchored proteins into the mitochondrial outer membrane does not require any known import components. *J. Cell Sci.* **121**, 1990-1998.

Lueder, F. and Lithgow, T. (2009). The three domains of the mitochondrial outer membrane protein Mim1 have discrete functions in assembly of the TOM complex. *FEBS Lett.* **583**, 1475-1480.

Meineke, B., Engl, G., Kemper, C., Vasiljev-Neumeyer, A., Paulitschke, H. and Rapaport, D. (2008). The outer membrane form of the mitochondrial protein Mcr1 follows a TOM-independent membrane insertion pathway. *FEBS Lett.* **582**, 855-860.

Mnaimneh, S., Davierwala, A. P., Haynes, J., Moffat, J., Peng, W. T., Zhang, W., Yang, X., Pootoolal, J., Chua, G., Lopez, A. et al. (2004). Exploration of essential gene functions via titratable promoter alleles. *Cell* **118**, 31-44.

Neupert, W. and Herrmann, J. M. (2007). Translocation of proteins into mitochondria. *Annu. Rev. Biochem.* **76**, 723-749.

Olsen, J. V., de Godoy, L. M., Li, G., Macek, B., Mortensen, P., Pesch, R., Makarov, A., Lange, O., Horning, S. and Mann, M. (2005). Parts per million mass accuracy on an Orbitrap mass spectrometer via lock mass injection into a C-trap. *Mol. Cell. Proteomics* **4**, 2010-2021.

Olsen, J. V., Nielsen, M. L., Damoc, N. E., Griep-Raming, J., Moehring, T., Makarov, A., Schwartz, J., Horning, S. and Mann, M. (2009). Characterization of the Velos, an enhanced LTQ orbitrap, for proteomics. *Mol. Cell. Proteomics* **8**, S40-S41.

Ong, S. E., Blagoev, B., Kratchmarova, I., Kristensen, D. B., Steen, H., Pandey, A. and Mann, M. (2002). Stable isotope labeling by amino acids in cell culture, SILAC, as a simple and accurate approach to expression proteomics. *Mol. Cell. Proteomics* **1**, 376-386.

Otera, H., Taira, Y., Horie, C., Suzuki, Y., Suzuki, H., Setoguchi, K., Kato, H., Oka, T. and Mihara, K. (2007). A novel insertion pathway of mitochondrial outer membrane proteins with multiple transmembrane segments. *J. Cell Biol.* **179**, 1355-1363.

Papic, D., Krumpe, K., Dukanovic, J., Dimmer, K. S. and Rapaport, D. (2011). Multispan mitochondrial outer membrane protein Ugo1 follows a unique Mim1-dependent import pathway. *J. Cell Biol.* **194**, 397-405.

Perkins, D. N., Pappin, D. J., Creasy, D. M. and Cottrell, J. S. (1999). Probability-based protein identification by searching sequence databases using mass spectrometry data. *Electrophoresis* **20**, 3551-3567.

Popov-Celeketić, J., Waizenegger, T. and Rapaport, D. (2008). Mim1 functions in an oligomeric form to facilitate the integration of Tom20 into the mitochondrial outer membrane. *J. Mol. Biol.* **376**, 671-680.

Rojo, M., Legros, F., Chateau, D. and Lombès, A. (2002). Membrane topology and mitochondrial targeting of mitofusins, ubiquitous mammalian homologs of the transmembrane GTPase Fzo. *J. Cell Sci.* **115**, 1663-1674.

Schägger, H., Cramer, W. A. and von Jagow, G. (1994). Analysis of molecular masses and oligomeric states of protein complexes by blue native electrophoresis and isolation of membrane protein complexes by two-dimensional native electrophoresis. *Anal. Biochem.* **217**, 220-230.

Schmitt, S., Prokisch, H., Schlunck, T., Camp, D. G., 2nd, Ahting, U., Waizenegger, T., Scharfe, C., Meitinger, T., Imhof, A., Neupert, W. et al. (2006). Proteome analysis of mitochondrial outer membrane from Neurospora crassa. *Proteomics* **6**, 72-80.

Selbach, M. and Mann, M. (2006). Protein interaction screening by quantitative immunoprecipitation combined with knockdown (QUICK). *Nat. Methods* **3**, 981-983.

Setoguchi, K., Otera, H. and Mihara, K. (2006). Cytosolic factor- and TOM-independent import of C-tail-anchored mitochondrial outer membrane proteins. *EMBO J.* **25**, 5635-5647.

Thornton, N., Stroud, D. A., Milenkovic, D., Guiard, B., Pfanner, N. and Becker, T. (2010). Two modular forms of the mitochondrial sorting and assembly machinery are involved in biogenesis of alpha-helical outer membrane proteins. *J. Mol. Biol.* **396**, 540-549.

Vermeulen, M., Eberl, H. C., Matarese, F., Marks, H., Denissov, S., Butter, F., Lee, K. K., Olsen, J. V., Hyman, A. A., Stunnenberg, H. G. et al. (2010). Quantitative interaction proteomics and genome-wide profiling of epigenetic histone marks and their readers. *Cell* **142**, 967-980.

Wach, A., Brachat, A., Pöhlmann, R. and Philippsen, P. (1994). New heterologous modules for classical or PCR-based gene disruptions in Saccharomyces cerevisiae. *Yeast* **10**, 1793-1808.

Wach, A., Brachat, A., Alberti-Segui, C., Rebischung, C. and Philippsen, P. (1997). Heterologous HIS3 marker and GFP reporter modules for PCR-targeting in Saccharomyces cerevisiae. *Yeast* **13**, 1065-1075.

Waizenegger, T., Stan, T., Neupert, W. and Rapaport, D. (2003). Signal-anchor domains of proteins of the outer membrane of mitochondria: structural and functional characteristics. *J. Biol. Chem.* **278**, 42064-42071.

Waizenegger, T., Schmitt, S., Zivkovic, J., Neupert, W. and Rapaport, D. (2005). Mim1, a protein required for the assembly of the TOM complex of mitochondria. *EMBO Rep.* **6**, 57-62.

Walther, D. M. and Rapaport, D. (2009). Biogenesis of mitochondrial outer membrane proteins. *Biochim. Biophys. Acta* **1793**, 42-51.

Walther, D. M., Papic, D., Bos, M. P., Tommassen, J. and Rapaport, D. (2009). Signals in bacterial beta-barrel proteins are functional in eukaryotic cells for targeting to and assembly in mitochondria. *Proc. Natl. Acad. Sci. USA* **106**, 2531-2536.

Walther, T. C. and Mann, M. (2010). Mass spectrometry-based proteomics in cell biology. *J. Cell Biol.* **190**, 491-500.

Wattenberg, B. and Lithgow, T. (2001). Targeting of C-terminal (tail)-anchored proteins: understanding how cytoplasmic activities are anchored to intracellular membranes. *Traffic* **2**, 66-71.

Westermann, B. and Neupert, W. (2000). Mitochondria-targeted green fluorescent proteins: convenient tools for the study of organelle biogenesis in Saccharomyces cerevisiae. *Yeast* **16**, 1421-1427.

Wiśniewski, J. R., Zougman, A., Nagaraj, N. and Mann, M. (2009). Universal sample preparation method for proteome analysis. *Nat. Methods* **6**, 359-362.

Zahedi, R. P., Sickmann, A., Boehm, A. M., Winkler, C., Zufall, N., Schönfisch, B., Guiard, B., Pfanner, N. and Meisinger, C. (2006). Proteomic analysis of the yeast mitochondrial outer membrane reveals accumulation of a subclass of preproteins. *Mol. Biol. Cell* **17**, 1436-1450.